

**Cell Reports, Volume 24**

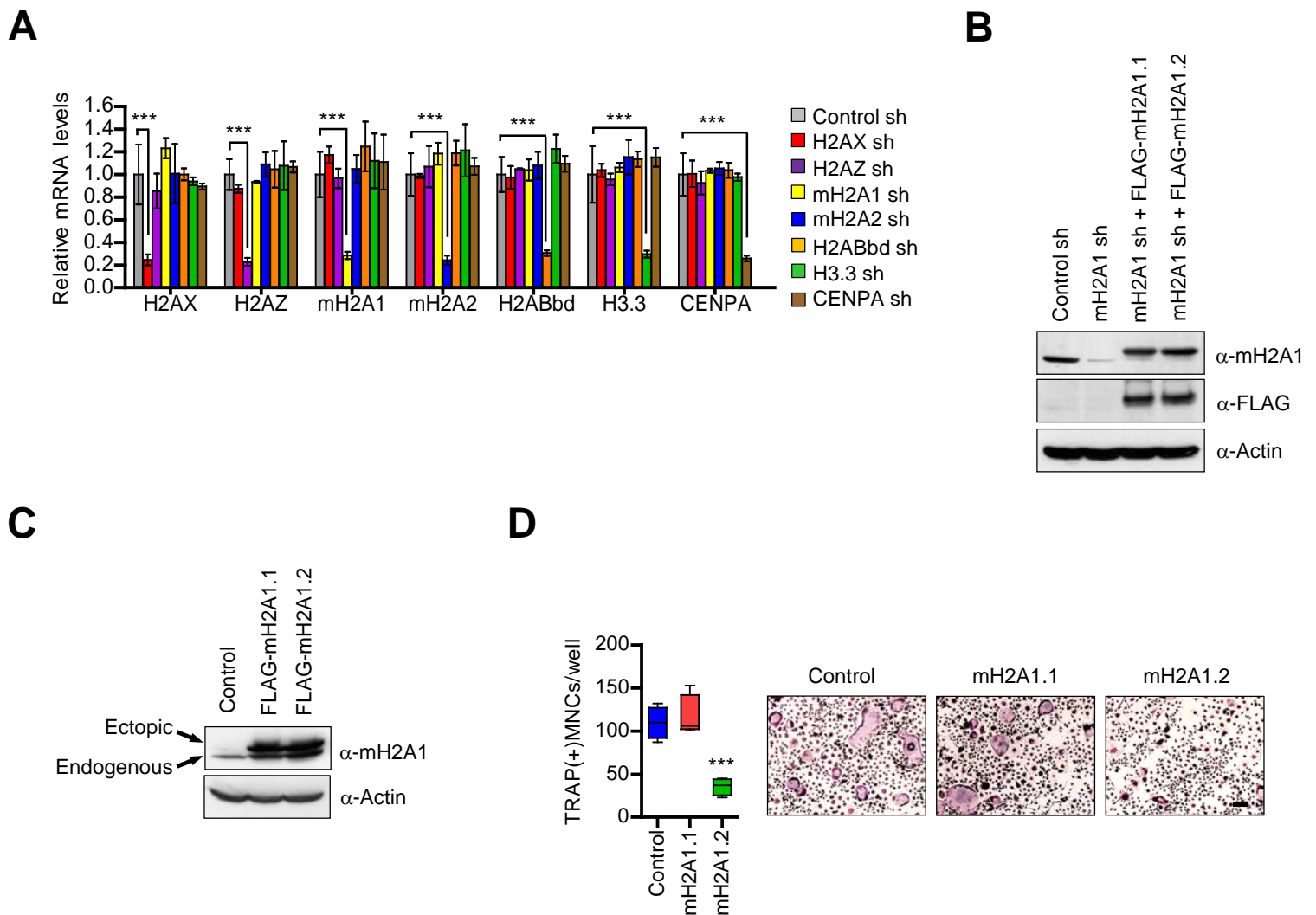
**Supplemental Information**

**Regulation of Breast Cancer-Induced**

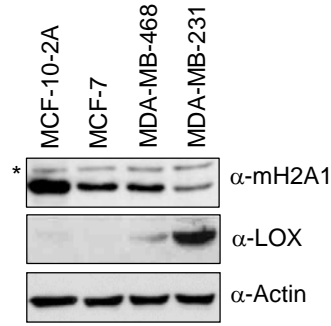
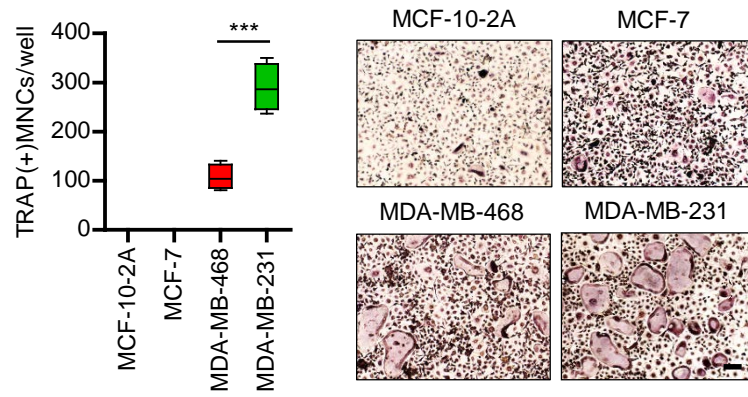
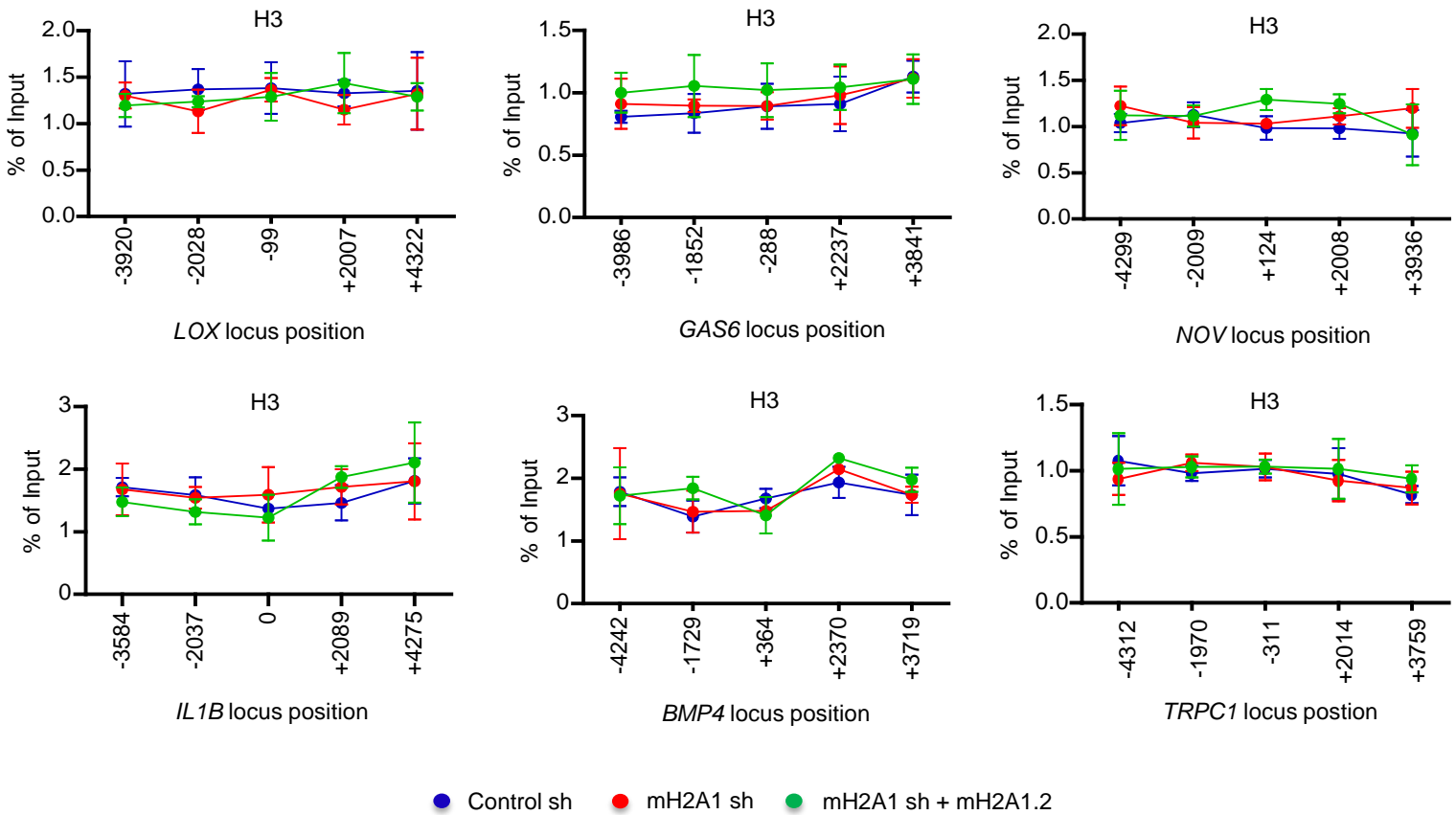
**Osteoclastogenesis by MacroH2A1.2**

**Involving EZH2-Mediated H3K27me3**

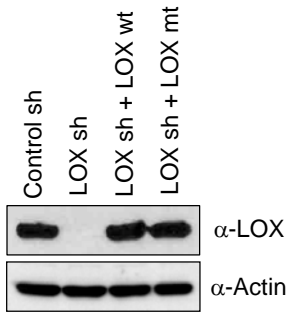
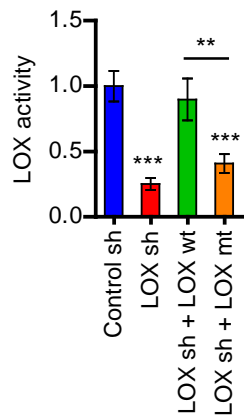
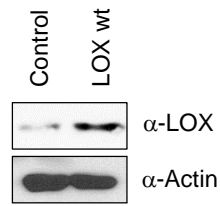
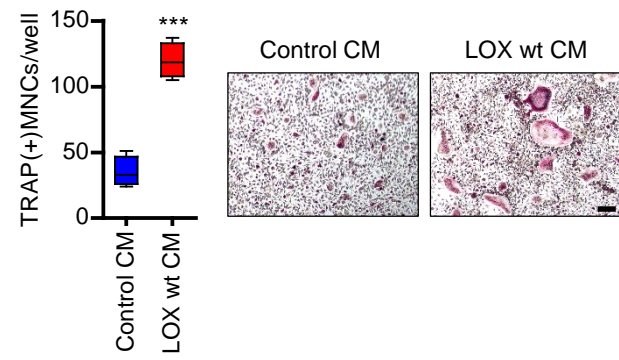
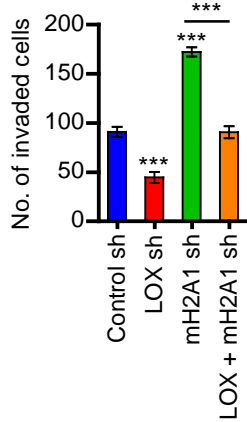
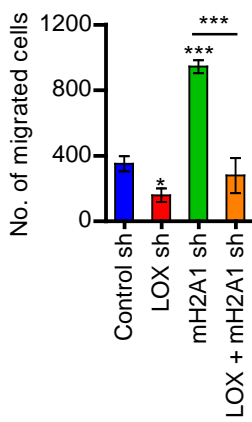
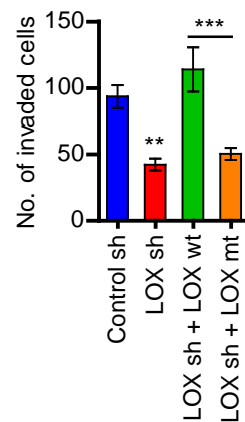
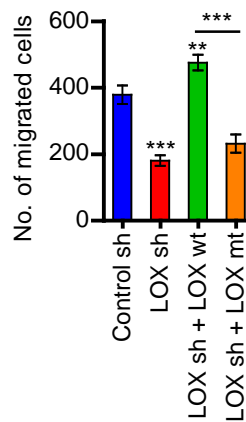
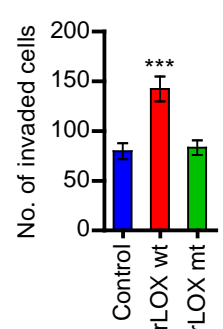
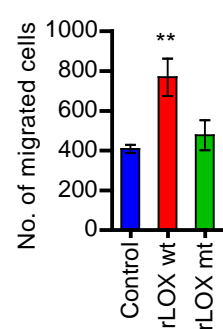
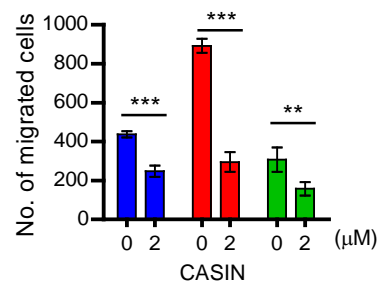
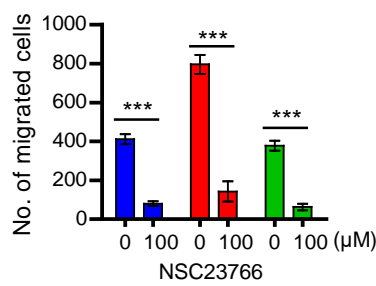
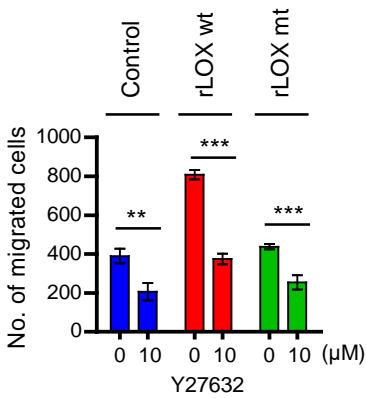
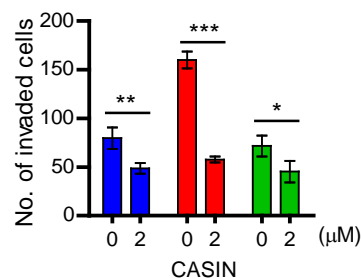
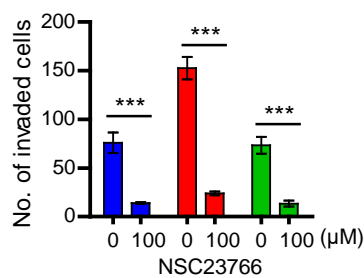
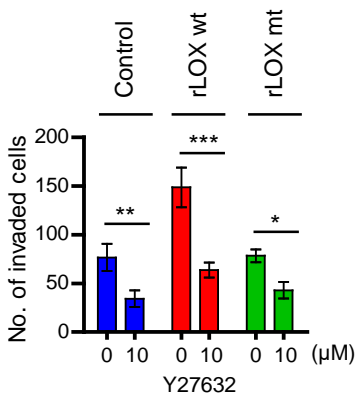
**Jinman Kim, Yonghwan Shin, Sunyoung Lee, Miyeong Kim, Vasu Punj, Jason F. Lu, Hongin Shin, Kyunghwan Kim, Tobias S. Ulmer, Jungmin Koh, Daewon Jeong, and Woojin An**



**Figure S1. Validation of Knockdown/Re-expression and Osteoclastogenic Effects of mH2A1.2-Transfected cell CMs. Related to Figure 1.** (A) MDA-MB-468 breast cancer cells were transduced with the indicated lentiviral shRNAs, and knockdown efficiency and specificity were determined by qRT-PCR with primers listed in Supplemental information. Error bars represent the means  $\pm$  SD ( $n = 3$ ); \*\*\* $P < 0.001$  versus Control sh (ANOVA analysis). (B) Whole cell extracts were prepared from mH2A1-depleted MDA-MB-468 cells transfected with FLAG-mH2A1.1 or FLAG-mH2A1.1, and analyzed by Western blot using mH2A1, FLAG and  $\beta$ -Actin antibodies. (C) Western blot analysis showing comparable expression of ectopic mH2A1.1 and mH2A1.2 in MDA-MB-468 cells. (D) OCP cells were treated with CMs from control or mH2A1/mH2A2-transfected MDA-MB-468 cells for 6 days and stained for TRAP to analyze osteoclast differentiation. Scale bar, 100  $\mu$ m. Error bars represent the means  $\pm$  SD ( $n = 4$ ); \*\*\* $P < 0.001$  versus Control (ANOVA analysis).

**A****B****C**

**Figure S2. mH2A1 and LOX Expression Levels in Breast Cell Lines and H3 Levels at mH2A1.2 Target Genes. Related to Figure 2.** (A) Whole cell lysates were prepared from MCF-10-2A, MCF-7, MDA-MB-468 and MDA-MB-231 cells, and analyzed by Western blot using mH2A1 and LOX antibodies. The asterisk indicates non-specific bands. (B) Osteoclastogenic properties of CMs from MCF-10-2A, MCF-7, MDA-MB-468 and MDA-MB-231 cells were measured by TRAP staining. Scale bar, 100 μm. Error bars represent the means ± SD (n = 4); \*\*\*P<0.001 (ANOVA analysis). (C) ChIP assays on mock-depleted or mH2A1-depleted MDA-MB-468 cells complemented with shRNA-resistant mH2A1.2 were performed to assess the levels of H3 at the *LOX*, *GAS6*, *NOV*, *IL1B*, *BMP4*, *TRPC1* genes. Error bars represent the means ± SD (n = 3).

**A****B****C****D****E****F****G****H****I**

**Figure S3. Effects of LOX Knockdown, rLOX Treatment, and Rho GTPase Inhibitor Treatment.**

**Related to Figure 3 .** (A) Western blot analysis for ectopic expression of LOX wild type (wt) and oxidase-dead mutant (mt) in LOX-depleted MDA-MB-468 cells. (B) LOX enzymatic activity in CMs from EZH2-depleted MDA-MB-468 cells expressing EZH2 wild type (wt) or methyltransferase-dead mutant (mt) was measured by using LOX activity assay kits. Error bars represent the means  $\pm$  SD ( $n = 3$ ); \*\*\* $P < 0.001$  versus Control sh (ANOVA analysis). (C) Western blot showing the expression of LOX wild type (LOX wt) transfected into MCF-7 cells. (D) OCP cells were treated with CMs from control or LOX-overexpressed MCF-7 cell for 6 days and osteoclast formation was determined by TRAP staining. Scale bar, 100  $\mu$ m. Error bars represent the means  $\pm$  SD ( $n = 4$ ); \*\*\* $P < 0.001$  (Student's *t*-test). (E) For migration assays (left), OCP cells treated with CMs from MDA-MB-468 cells depleted of LOX and/or mH2A1 were seeded and incubated for 5 h in transwell inserts for migration. For invasion assays (right), MDA-MB-468 cells depleted of LOX and/or mH2A1 were seeded into upper chamber coated with Matrigel, and then allowed to invade to culture media containing 10% FBS for 48 h. The migrated and invaded cells were stained and photographed, and the number of cells that had invaded or migrated to the other pole of the membrane was counted under a light microscope. (F) Cell migration and invasion assays were performed as in (E), but LOX-depleted MDA-MB-468 cells expressing LOX wild type (wt) and mutant (mt) and their CMs were used. (G) Cell migration and invasion assays were performed as in (E), but using wild type (wt) or mutant (mt) rLOX-transfected MDA-MB-468 cells and their CMs. Error bars in (E-G) represent the means  $\pm$  SD ( $n = 3$ ); \* $P < 0.05$ , \*\* $P < 0.01$ , \*\*\* $P < 0.001$  versus Control sh CM or Control (ANOVA analysis). (H) The lower side of transwell filters was coated with rLOX wt or mt in MDA-MB-468 CMs for 16 h. OCP cells were detached and seeded into the upper chamber of transwell filters, and then allowed to adhere for 1 h. Y27632 (RhoA inhibitor), NSC23766 (Rac1 inhibitor), and CASIN (Cdc42 inhibitor) were added to the lower chamber and then allowed to further migrate for 5 h. (I) MDA-MB-468 cells were detached and resuspended in culture media containing rLOX wt or mt. The suspended cells were pretreated with Y27632, NSC23766, or CASIN, seeded onto the upper chamber coated with Matrigel, and then allowed to invade for 48 h. Error bars in (H) and (I) represent the means  $\pm$  SD ( $n = 3$ ); \* $P < 0.05$ , \*\* $P < 0.01$ , \*\*\* $P < 0.001$  (ANOVA analysis).

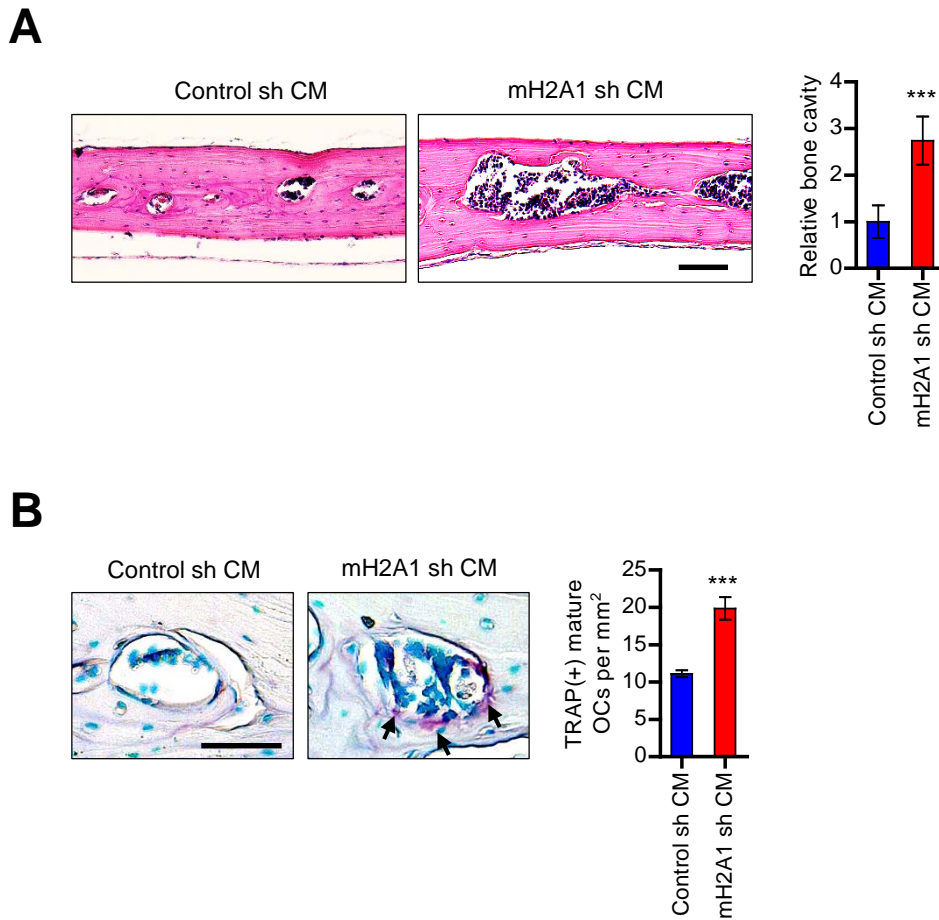


**Figure S4. In Vivo Osteoclastogenic Effects of CMs Collected from mH2A1-Depleted Cells. Related to Figure 4.** CMs were prepared from control shRNA or mH2A1 shRNA-infected MDA-MB-468 cells and concentrated 10-fold with a 10-kDa cut-off centrifugal filter. Calvarial bones of C57BL/6 female mice were injected with CMs (100  $\mu$ l) from mock-depleted (Control sh CM) or mH2A1-depleted (mH2A1 sh CM) MDA-MB-468 cells. Calvarial bones were fixed, embedded, and stained for H&E (A) and TRAP (B). Representative images of H&E and TRAP staining are shown on the left (scale bar, 100  $\mu$ m). Quantification of osteolytic lesion formation and TRAP positive mature osteoclasts is shown on the right. Arrows point to TRAP+ mature osteoclasts. Error bars represent the means  $\pm$  SD ( $n = 5$ ); \*\*\* $P < 0.001$  versus Control sh CM (Student's  $t$ -test).

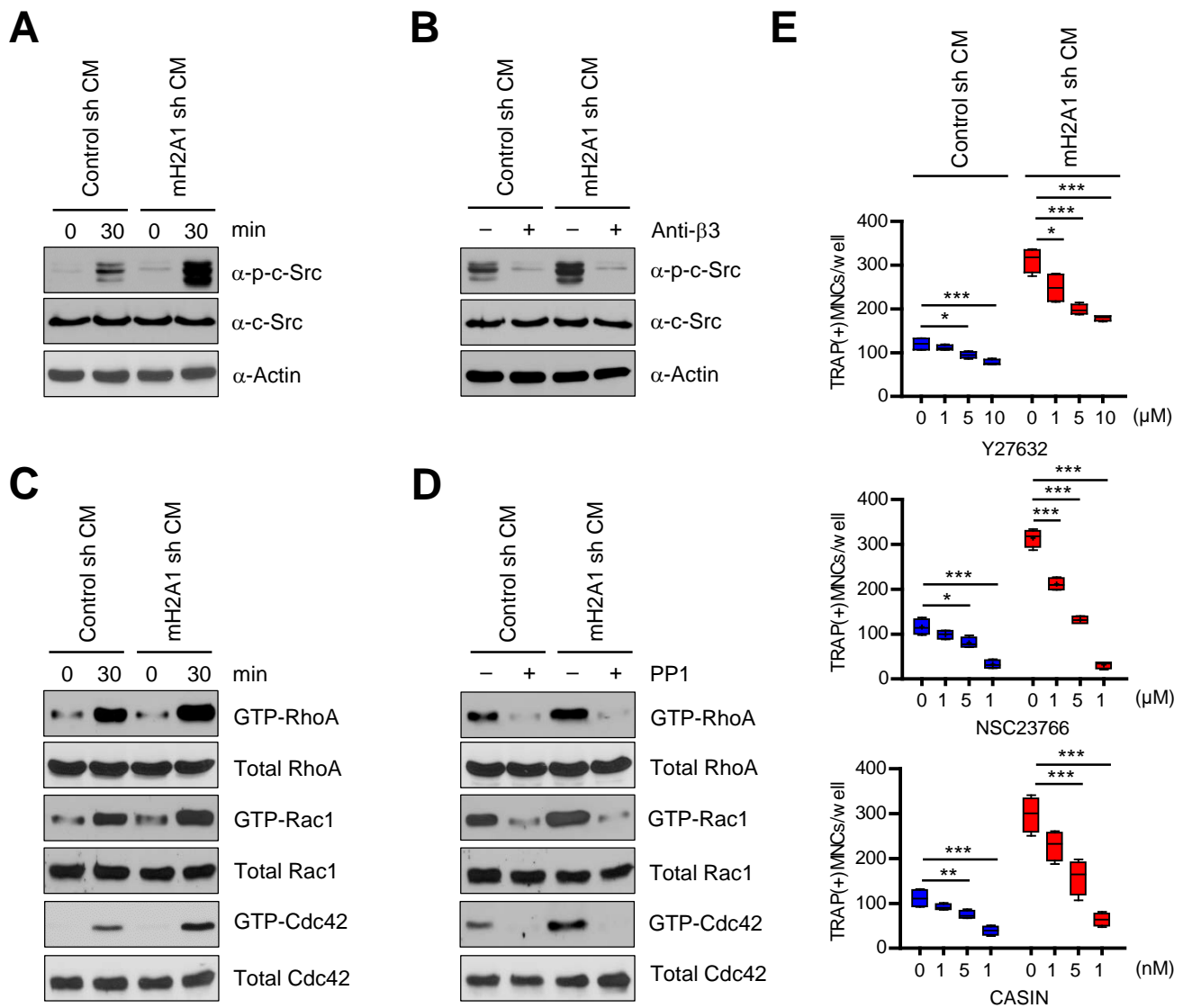


**Figure S5. Effects of mH2A1-Depleted MDA-MB-468 CMs on c-Src and small GTPase Signaling.**

**Related to Figure 5.** (A) OCP cells were incubated with M-CSF (15 ng/ml) and RANKL (15 mg/ml) for 3 days and treated with CMs collected from control or mH2A1-depleted MDA-MB-468 cells for 24 h. After M-CSF/RANKL starvation for 4 h, cells were detached and resuspended in  $\alpha$ -MEM with 0.5% FBS. The cells were seeded onto culture dishes coated with control or mH2A1-depleted MDA-MB-468 CMs and cultured for 30 min. The cells were lysed and subjected to Western blot with antibodies against c-Src and phosphorylation of c-Src.  $\beta$ -Actin was used as a loading control. (B) OCP cells were detached, resuspended, and pretreated with integrin  $\beta$ 3 blocking antibody for 15 min. The cells were plated into dishes coated with CMs from control or mH2A1-depleted MDA-MB-468 cells and incubated for 30 min. Cell lysates were then prepared and analyzed by Western blot with phospho-c-Src and c-Src antibodies.  $\beta$ -Actin was used as a loading control. (C) RhoA/Rac1/Cdc42 GTPases assays were done as described in Experimental Procedures, and whole cell lysates were analyzed by Western blot. (D) Small GTPases assays were performed as in (B), but using PP1 (Src inhibitor). (E) OCP cells were incubated with CMs from control or mH2A1-depleted MDA-MB-468 cells in the presence of the indicated inhibitors (RhoA inhibitor Y27632, Rac1 inhibitor NSC23766, or Cdc42 inhibitor CASIN) for 6 days. Mature osteoclasts were TRAP-stained and counted. Error bars represent the means  $\pm$  SD ( $n = 4$ ); \* $P < 0.05$ , \*\* $P < 0.01$ , \*\*\* $P < 0.001$  (ANOVA analysis).

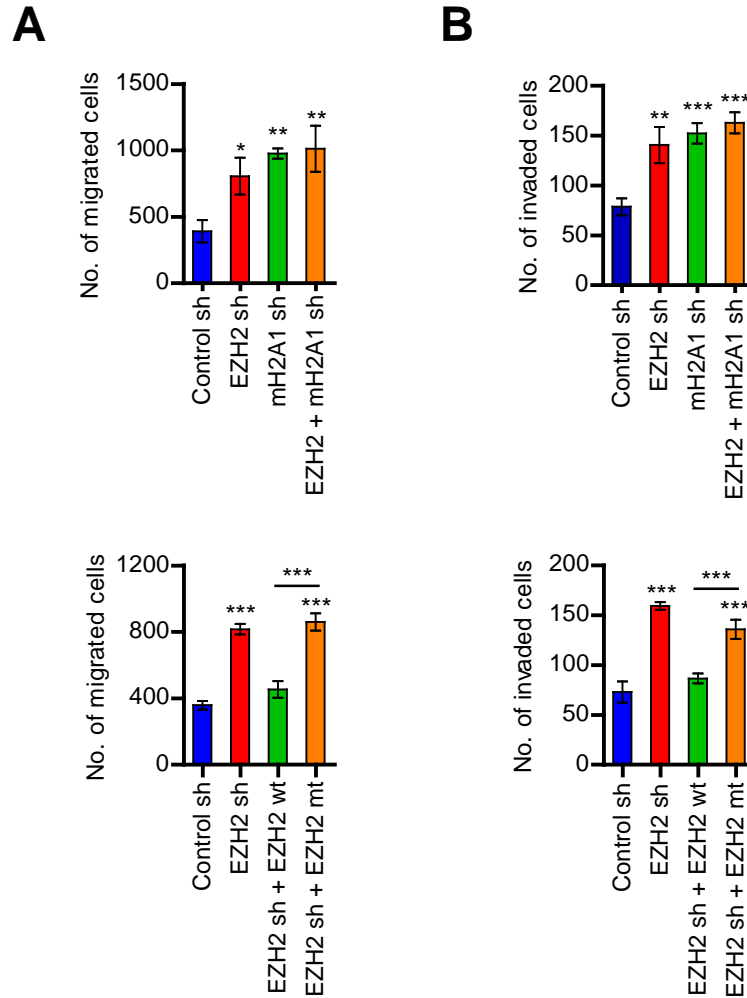


**Figure S6. Effects of Soluble Factors Released by EZH2-depleted Cells on OCP Cell Migration and MDA-MB-468 Cell Invasion. Related to Figure 7.** (A) OCP cells were treated with CMs from MDA-MB-468 cells depleted of EZH2 and/or mH2A1, and subjected to cell migration assays (upper). CMs from EZH2-depleted MDA-MB-468 cells expressing EZH2 wild type (wt) or enzymatically dead mutant (mt) were also used for assays (lower). (B) MDA-MB-468 cells were depleted of EZH2 and/or mH2A1 and applied to cell invasion assays (upper). Cell invasion assays were also performed with EZH2-depleted cells expressing EZH2 wt or mt (lower). Error bars in (A) and (B) represent the means  $\pm$  SD ( $n = 3$ ); \* $P < 0.05$ , \*\* $P < 0.01$ , \*\*\* $P < 0.001$  versus Control sh CM (ANOVA analysis).



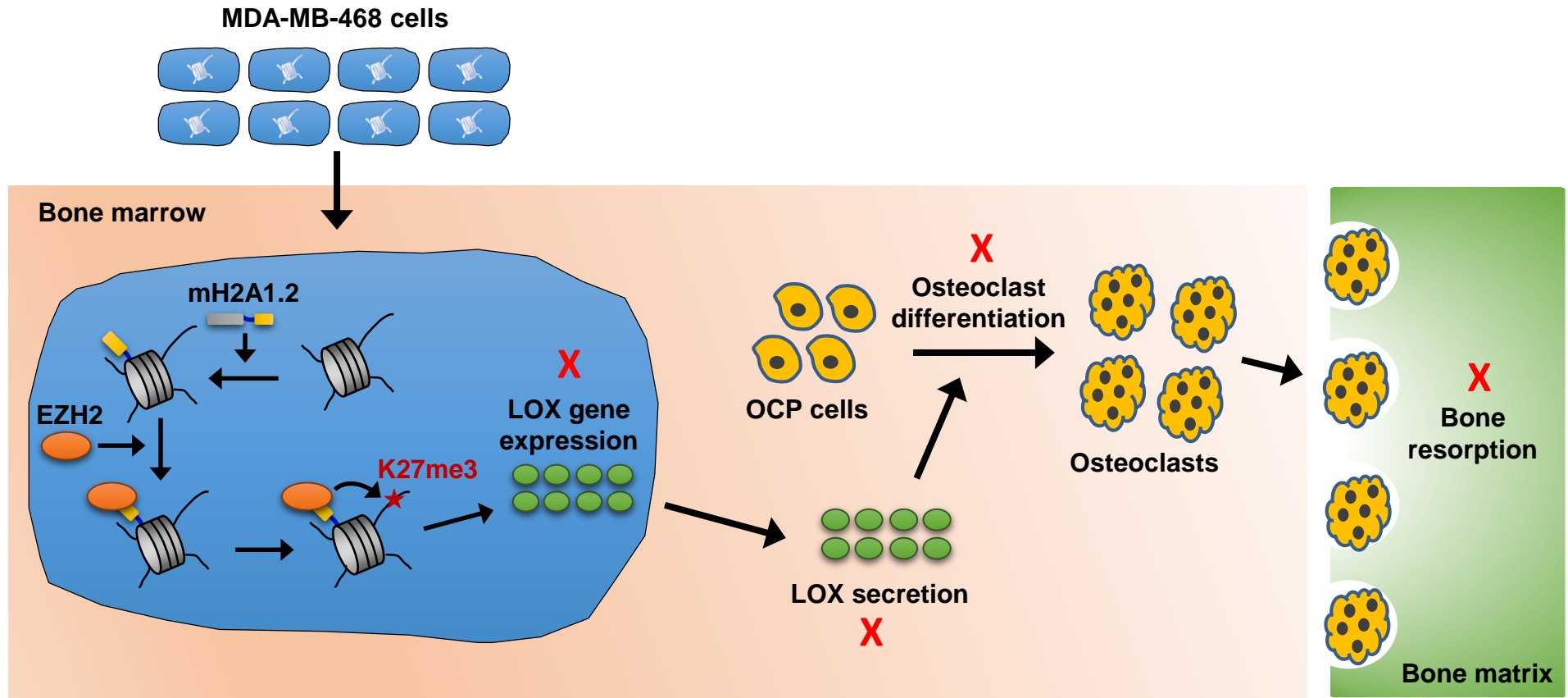


**Figure S7. Model for the Cooperative Role of mH2A1.2 and EZH2-Mediated H3K27me3 in Regulating LOX Expression and Osteoclastogenesis. Related to Figure 1-7. See DISCUSSION for more details.**

## SUPPLEMENTAL EXPERIMENTAL PROCEDURES

### RNAi, ChIP, and qRT-PCR

DNA oligonucleotides encoding shRNAs specific for the 3'UTR or CDS regions of histone variants, LOX and EZH2 (listed in Table S1) were subcloned into pLKO.1 lentiviral expression vector (Addgene) according to standard procedures (<https://www.addgene.org/tools/protocols/plko/>). Lentiviral particles were generated in 293T cells by co-transfecting plasmids encoding VSV-G, NL-BH and the shRNAs. MDA-MB-468 breast cancer cells were infected with these viruses and selected with puromycin (2 µg/ml) for two weeks. ChIP assays were performed using mH2A1 and EZH2 antibodies and the ChIP assay kit (Millipore) as previously described (Kim et al., 2016b). DNA molecules immunoprecipitated from MDA-MB-468 cells were analyzed by qPCR using the primers that amplify the five different regions extending over 8 kb including approximately 4 kb upstream and 4 kb downstream of transcription start sites of the *LOX*, *GAS6*, *NOV*, *IL1B*, *BMP4*, and *TRPC1* genes. The primers used for qPCR are listed in Table S4. All qPCR reactions were run in triplicate, and specificity of amplification was determined by melting curve analysis. For qRT-PCR, total RNA was isolated from MDA-MB-468 cells using an RNeasy mini kit (Qiagen). After converting RNA to cDNA using iScript cDNA Synthesis Kit (Bio-Rad), real-time RT-PCR was performed using one-step QuantiTect SYBR Green RT-PCR kit (Qiagen) according to the manufacturer's instructions. The primers used quantitative real-time PCR are listed in the Table S4.

### Constructs and Antibodies

Bacterial expression constructs of mH2A1.2 and EZH2 were generated by PCR-amplifying and sub-cloning their cDNAs into pGEX-4T1 and pET15b vectors. For mammalian expression of H2A, mH2A1.1, mH2A1.2, LOX and EZH2, the corresponding cDNAs were amplified by PCR and ligated into the correct reading frames of lentiviral expression vector pLenti-Hygro (Addgene) containing 5' FLAG coding sequences. To prepare lentiviral particles for H2A, mH2A1.1, mH2A1.2, LOX and EZH2, 293T cells were transfected with plasmids encoding VSV-G, NL-BH and the pLenti-Hygro constructs (H2A, mH2A1.1, mH2A1.2, LOX and EZH2) using Lipofectamine 2000 (Invitrogen). MDA-MB-468 breast cancer cells stably expressing the pLenti-Hygro constructs were generated by lentivirus infection and subsequent selection for Hygromycin B (200 µg/ml, Invitrogen) resistance for two weeks. To generate shRNA-resistant mH2A1.1 and mH2A1.2 expression vectors, wild type mH2A1.1 and mH2A1.2 constructs were point-mutated by the QuikChange® II site-directed mutagenesis kit according to manufacturer's protocol (Agilent Technologies). Further details of plasmid constructions are available upon request. The following antibodies were used in this study: Cathepsin K (cat.no. ab19027), H3

(cat.no. ab1791), H3K4me1 (cat.no. ab176877), H3K4me3 (cat.no. ab8580), H3K36me1 (cat.no. ab9048), and H3K36me3 (cat.no. ab9050) antibodies from Abcam,  $\beta$ -Actin (cat.no. A5441), FLAG (cat.no. F1804), and HA (cat.no. H3663) antibodies from Sigma-Aldrich, His (cat.no. LT0426) antibody from Lifetein, EZH2 (cat.no. 39901), H3ac (cat.no. 61637), H4ac (cat.no. 39925), H3K9me3 (cat.no. 39161), and H3K27me1 (cat.no. 61015) antibodies from Active Motif, ATP6V0D2 (cat.no. sc-69111), c-Src (cat.no. sc-19), GST (cat.no. sc-138), and NFATc1 (cat.no. sc-13033) antibodies from Santa Cruz Biotechnology, Cdc42 (cat.no. 240201), RhoA (cat.no. 240302), and Rac1 (cat.no. 240106) antibodies from Cell Biolabs, p-c-Src (Tyr416) (cat.no. 2101) antibody from Cell Signaling, and H2Aac (cat.no. 07-376), H2Bac (cat.no. 07-373), H3K4me2 (cat.no. 07-030), H3K9me1 (cat.no. 07-450), H3K9me2 (cat.no. 07-441), H3K27me2 (cat.no. 07-452), H3K27me3 (cat.no. 07-449), H3K36me2 (cat.no. 07-369), Integrin  $\beta$ 3 (cat.no. MAB2023Z) and LOX (cat.no. ABT112) antibodies from Millipore.

### **Generation of Breast Cancer Secretome**

To generate a breast cancer secretome, we used the secretory protein accession numbers from the expressed genes from various databases as well as published studies as summarized in Supplementary Table S2. Within each secretome source database, only human specific proteins were searched. Protein IDs or hugo gene names were interconverted to unique gene IDs using BiodBnet (<https://biodbnet-abcc.ncifcrf.gov/>) and DAVID (<http://david.abcc.ncifcrf.gov/conversion.jsp>). A subset of proteins with a predicted signal peptide and experimentally confirmed to be secretory or localized in membrane were created. All identified secretory proteins were mapped to genes corresponding to GRCh37. Mapping of these identified proteins on Illumina transcriptome Human HT-12 V4 expression ChIP identified a subset of 6,267 candidate probes, which represents 'secretome array' of breast in the present study. To avoid any redundancy, further analysis was performed with the 6,267 probes (or 3948 genes) including genes encoding breast specific secretory proteins.

### **Tissue qPCR Array**

TissueScan Breast Cancer and Normal Tissue cDNA array (BCRT102/302/502) was obtained from Origene Technologies. The array contained a panel of dried cDNAs from 48 samples including five normal samples. The expression of mH2A1.2 and LOX was measured by using SYBR Green PCR kit (Qiagen). A description in depth pathology report (including histology sections) for all of the RNA molecules used in the panel can be viewed in Table S5 and OriGene's Website.

### **Cell Migration and Invasion Assay**

For migration assays, the lower side of transwell filters was coated with rLOX wt (100 ng/ml) or LOX mt (100 ng/ml) in the presence of MDA-MB-468 CMs for 16 h and then blocked with 1% BSA for 1 h. OCP cells ( $1 \times 10^5$  cells) were seeded onto the upper chamber of transwell filters in  $\alpha$ -MEM containing 0.5% FBS. After rLOX wt or rLOX mt were added to the lower chamber in  $\alpha$ -MEM culture medium containing M-CSF (15 ng/ml) and RANKL (15 ng/ml), cells were allowed to migrate to lower chamber for 5 h. For invasion assays, the transwell filters were coated with Matrigel (BD Biosciences) for 1h. MDA-MB-468 cells ( $1 \times 10^5$  cells) were detached and resuspended in DMEM containing 0.5% FBS, rLOX wt (100 ng/ml), or rLOX mt (100 ng/ml), and then seeded onto the upper chamber of transwell filters. The culture media in the lower chamber contained 10% FBS, rLOX wt or rLOX mt. The cells were allowed to invade for 48 h. The invaded or migrated cells were fixed with 3.7% formalin for 15 min, stained with 1% crystal violet for 1 h, and photographed. For each experiment, pictures of 5 fields (equal size) were taken and the cells have been counted.

### **LOX Enzyme Activity Assay**

LOX activity in the conditioned media (50  $\mu$ l) was measured by using a LOX activity assay kit according to manufacturer's instructions (Abcam). Samples were placed on ice and changes in fluorescence were measured using a fluorescence spectrophotometer with excitation and emission wavelengths 540 and 590 nm respectively. The level of hydrogen peroxide generated by LOX enzymatic activity was determined by comparing fluorescence changes to a standard plot, relating fluorescence change to nmoles of hydrogen peroxide added to assays lacking LOX. The value corresponding to the amount of hydrogen peroxide produced was then normalized to total protein.

### **RhoA/Rac1/Cdc42 GTPase and Western Blot Analysis**

The assays for measuring RhoA, Rac1, and Cdc42 GTPase activities were performed using RhoA/Rac1 assay kit according to manufacturer's protocol (Cell Biolabs). OCP cells were lysed with a lysis buffer (50 mM Tris-HCl, pH 7.5, 10 mM MgCl<sub>2</sub>, 150 mM NaCl, 2% NP40, and 1x Roche protease inhibitor cocktail). After centrifuging cell lysates, the supernatants were incubated with Rhotekin RBD agarose (Cell Biolabs) or PAK1 PBD agarose (Cell Biolabs) for 2 h. The mixture was washed, re-suspended in lysis buffer, and applied to Western blotting. For Western blot analysis of c-Src and small GTPases (RhoA, Rac and Cdc42), OCP cells ( $1 \times 10^6$ /100-mm culture dish) were incubated with M-CSF (15 ng/ml) and RANKL (15 ng/ml) for 3 days and treated with rLOX (100 ng/ml) in 10% FBS for 24 h. After 4 h starvation of M-CSF, RANKL and rLOX in  $\alpha$ -MEM medium, cells were transferred to culture dishes

coated with rLOX in MDA-MB-468 CMs and cultured at 37°C over a 30-min time period. The cells were then lysed and subjected to Western blot analysis.

### **Bone Resorption Assay**

Osteoclasts were plated on dentin slices (IDS Ltd.), treated with rLOX wt or rLOX mt (100 ng/ml) in MDA-MB-468 CMs containing M-CSF (30 ng/ml) and RANKL (30 ng/ml), and further cultured for 48 h to resorb bone. Dentine slices were then ultrasonicated to remove adherent cells, and resorption pits on the slice were stained with 1% toluidine blue. The resorbed area was analyzed using Image-Pro Plus program (MediaCybernetics).

### **cDNA Microarray Analysis**

Total RNA was extracted from mock- or mH2A1-depleted MDA-MB-468 cells using the TRI-zol reagent (Invitrogen), and hybridized on whole-genome expression array (Human HT-12 v4 Expression BeadChip, Illumina). To detect differential expression of genes corresponding to secreted factors, microarray data were background corrected with GenomeStudio based on manufacturer's recommendation and normalized using limma package (Ritchie, et al., 2015). Probe level data were summarized into a single expression value for each gene, and were further analyzed with 3948 candidate virtual secretome genes. Differences in mRNA levels between control and mH2A1-depleted cells were determined using strict statistical criteria of detection p-value in all replicates  $p < 0.05$ . The gene expression array data have been deposited in the NCBI Gene Expression Omnibus (GEO) database under the GEO accession number GSE107570.

### **Pathway-Based Approach for Secretory Biomarker Discovery and Candidate Gene Prioritization**

To study the potential functional significance of all secretome genes, we queried different signature databases such as Gene ontology, Mammalian phenotype, Pathway, Protein domain, PubMed, Protein Interaction, and Gene Expression. Hypergeometric distribution along with Benjamini Hochberg correction was used as the standard method for determining p value of significance. Further, fisher's inverse chi-square method was used to combine p-values from multiple features/annotations into an overall P-value to rank the genes with each pathway ( $p < 0.05$ ). A functional annotation-based candidate gene prioritization approach based on a fuzzy-based similarity between two genes in semantic annotations was used as described previously (Kaimal et al., 2011; Punj et al., 2012). This approach uses a protein interaction database derived from the entire Medline abstract database. Such analysis was aimed to explore the global and systemic properties of the biomarker underlying molecular networks of the

biomarker and enables interpretation of the biologic significance of the gene list. This annotation was used to prioritize candidate biomarkers for validation.

### **Purification and Analysis of Nucleosomes**

Nuclear pellets were prepared from MDA-MB-468 cells transfected with FLAG-tagged H2A and mH2A1.2, and were digested with micrococcal nuclease in nuclear extraction buffer (20 mM HEPES, pH 7.4, 500 mM NaCl, 1.5 mM MgCl<sub>2</sub>, 0.2 mM EGTA, and 1x Roche protease inhibitor cocktail) to produce predominantly mononucleosomes. After adjusting the salt concentration of the reaction to 300 mM NaCl, ectopic H2A/mH2A1.2-containing nucleosomes were purified by immunoprecipitation on anti-FLAG antibody-conjugated agarose beads in washing buffer (20 mM HEPES, pH 7.8, 300 mM NaCl, 1.5 mM MgCl<sub>2</sub>, 0.2 mM EGTA, 10% Glycerol, 0.2% Triton X-100, and 1x Roche protease inhibitor cocktail). Bead-bound nucleosomes were analyzed by Western blot using antibodies against specific histone modifications.

### **Protein-Protein Interaction**

GST and GST-tagged proteins were expressed in *E. coli* Rosetta 2 (DE3) pLysS (Novagen) and purified on Glutathione-Agarose beads (Sigma-Aldrich) as described previously (Kim et al., 2015). In vitro binding assays were performed with equal amounts of GST or GST fusion proteins in affinity buffer (20 mM HEPES-KOH, pH 7.9, 0.5 mM EDTA, 200 mM NaCl, 10% glycerol, and 0.1% Nonidet P-40) supplemented with PMSF, DTT, and protease inhibitor mixture. Bound proteins were washed four times with affinity buffer, and detected by Western blotting. Ten percent of the interaction mix were loaded as an input fraction.

### **Co-Immunoprecipitation**

MDA-MB-468 breast cancer cells were lysed in cell lysis buffer (50 mM Tris-HCl, pH 7.4, 150 mM NaCl, 1 mM EDTA, and 1% Triton X-100) supplemented 1x Roche protease inhibitor cocktail. Cell lysate materials were pre-cleared for 1 h with A/G beads (Santa Cruz Biotechnology) and then incubated with mH2A1 and EZH2 antibodies overnight. As a negative control, normal IgG was used that showed negligible signal. The following day, A/G agarose beads were added to the immunoprecipitates for 1 h. After washing the beads four times with lysis buffer, the binding of endogenous mH2A1 and EZH2 was examined by Western blot.

### **Statistical Analysis**

All quantitative data are presented as mean  $\pm$  SD. Statistical analyses of datasets were performed with Student's two-tailed *t*-test or two-way ANOVA followed by Bonferroni's comparison test. GraphPad Prism (GraphPad Software Inc.) was used for all analyses. A *P* value  $< 0.05$  was considered statistically significant.

## SUPPLEMENTAL REFERENCES

Kaimal, V., Sardana, D., Bardes, E.E., Gudivada, R.C., Chen, J. and Jegga, A.G. (2011) Integrative systems biology approaches to identify and prioritize disease and drug candidate genes. *Methods. Mol. Biol.* *700*, 241-259.

Kim, H., Heo, K., Choi, J., Kim, K. and An, W. (2011). Histone variant H3.3 stimulates HSP70 transcription through cooperation with HP1gamma. *Nucleic Acids Res.* *39*, 8329-8341.

Kim, J.M., Heo, K., Choi, J., Kim, K. and An, W. (2013a). The histone variant MacroH2A regulates Ca(2+) influx through TRPC3 and TRPC6 channels. *Oncogenesis* *2*, e77.

Kim, J.M., Kim, K., Punj, V., Liang, G., Ulmer, T.S., Lu, W. and An, W. (2015). Linker histone H1.2 establishes chromatin compaction and gene silencing through recognition of H3K27me3. *Sci Rep* *5*, 16714.

Kim, J.M., Kim, K., Schmidt, T., Punj, V., Tucker, H., Rice, J.C., Ulmer, T.S. and An, W. (2015) Cooperation between SMYD3 and PC4 drives a distinct transcriptional program in cancer cells. *Nucleic Acids Res.* *43*, 8868-8883.

Kim, K., Punj, V., Choi, J., Heo, K., Kim, J.M., Laird, P.W. and An, W. (2013b). Gene dysregulation by histone variant H2A.Z in bladder cancer. *Epigenetics Chromatin* *6*, 34.

Kim, K., Punj, V., Kim, J.M., Lee, S., Ulmer, T.S., Lu, W., Rice, J.C. and An, W. (2016b). MMP-9 facilitates selective proteolysis of the histone H3 tail at genes necessary for proficient osteoclastogenesis. *Genes Dev* *30*, 208-219.

Punj, V., Matta, H. and Chaudhary, P.M. (2012) A computational profiling of changes in gene expression and transcription factors induced by vFLIP K13 in primary effusion lymphoma. *PLoS One* *7*, e37498.

Ritchie, M.E., Phipson, B., Wu, D., Hu, Y., Law, C.W., Shi, W. and Smyth, G.K. (2015) limma powers differential expression analyses for RNA-sequencing and microarray studies. *Nucleic Acids Res.* *43*, e47.